Source parameters of the Izmit-Bolu 1999 (Turkey) earthquake sequences from teleseismic data

Anastasia Kiratzi and Eleni Louvari
Geophysical Laboratory, Aristotle University of Thessaloniki, Greece

Abstract
Body waveform modelling and far-field displacement spectral analyses were used to study the source parameters of five of the largest earthquakes of the (Izmit-Bolu) Turkey 1999 sequence. The derived source parameters for the August 17, 1999 M_W 7.4 event are: strike = 267°, dip = 85°, rake = – 175°, h = 10 km, $M_0 = 1.31 \cdot 10^{20}$ Nm. The length of the fault was found equal to 76 km, the average displacement 6.4 m and the static stress drop 90 bars. The Bolu November 12, 1999 M_W 7.1 event has a focal mechanism with strike = 262°, dip = 53°, rake = –177°, h = 12 km, $M_0 = 4.71 \cdot 10^{19}$ Nm, fault length of 56 km, average displacement 2.1 m and average static stress drop 29 bars. The focal mechanisms of three other aftershocks of the Izmit sequence indicate right lateral strike slip motion, as well. The slip vectors of the events studied are in accordance with the GPS velocity vectors, have a mean azimuth of 269° and reveal the extrusion of the Anatolian plate towards the Aegean.

Key words *source inversion – complex earthquakes – North Anatolian Fault*

1. Introduction

The earthquake of August 17, 1999 was the strongest (M_w = 7.4) and most destructive to occur in Turkey since the 1939 Erzincan event. It occurred on the western branch of the North Anatolian Fault Zone (NAFZ) and the epicentre (40.76°N, 29.97°E, Kandili Observatory determination) was close to Izmit (fig. 1) at the eastern end of Izmit Bay. The earthquake devastated towns on the shores of Izmit Bay and Adapazari to the east. More than 15 350 people died, while 24 000 were injured. 50 000 buildings collapsed or were damaged beyond repair. In Istanbul, located 90 km west of the epicentre, 1 000 people were killed by the collapse of buildings. Three months later, on November 12, 1999, another strong M_w 7.1 earthquake occurred near Bolu (epicentre 40.79°N, 31.21°E Kandili Observatory determination), an area located at the eastern end of the August 17 rupture. This event has been reported to cause 650 casualties, 3300 people injured and 750 buildings destroyed.

The M_w 7.4 Izmit earthquake produced ~ 110 km of surface rupture, with up to 5 m of dextral slip, while the M_w 7.1 Bolu event produced ~40 km rupture it was also associated with a right lateral motion with up to 3.5-4.5 m offset (*U.S. Geol. Surv. 1999* - field reports).

The Izmit earthquake is the latest in a sequence of strong events, which have occurred this century and have ruptured a nearly 1000-km-long section of the NAFZ. It filled in a 100 to 150 km long gap between the 1967, 1963 and 1964 events. This gap was first noted by Toksöz *et al.* (1979) and its hazard was later analysed by Stein *et al.* (1997), who estimated there was

Mailing address: Assoc. Prof. Anastasia Kiratzi, Geophysical Laboratory, Aristotle University of Thessaloniki, GR 540 06 Thessaloniki, Greece; e-mail: kiratzi@geo.auth.gr

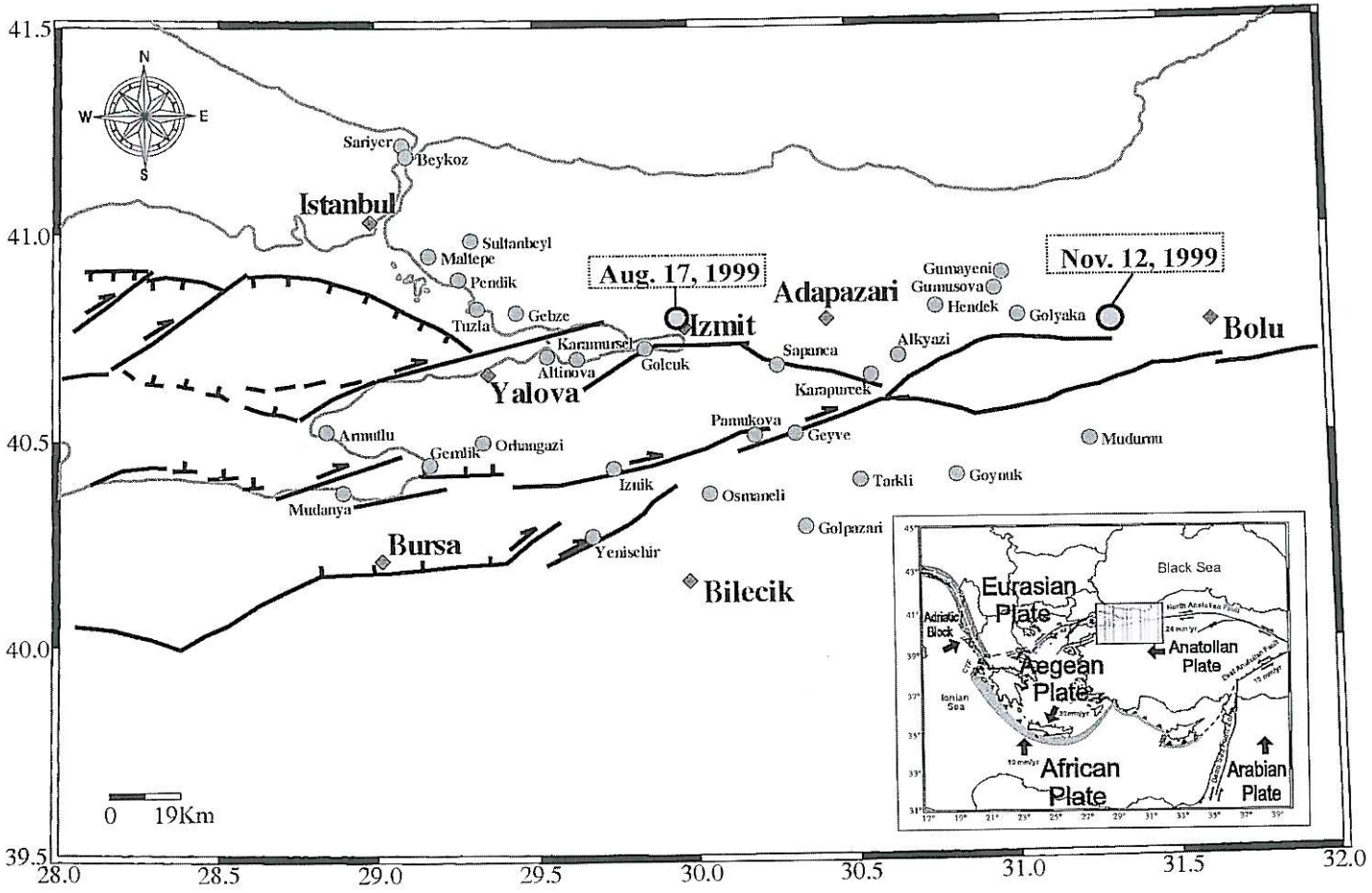

Fig. 1. A general location map showing major segments, as in Barka (1992), of the North Anatolian Fault Zone. The inset (from Papazachos *et al.*, 1998) shows the major plates involved and the area studied.

a 12% chance of this earthquake to occur in the 30 years from 1996 to 2026.

In the present paper we use teleseismic waveforms to invert for the focal mechanism for five of the largest earthquakes of the Izmit and Bolu sequences and determine the source properties of the two mainshocks, using far-field displacement spectral analysis.

2. Teleseismic waveform modelling and data used

The technique of body-waveform modelling, based on the algorithm of McCaffrey *et al.* (1991), was used to calculate the focal mechanism of the larger events of the sequences. The data used in the inversion consisted of *P* and *SH* broadband waveforms (all having a sampling frequency of 1 Hz), recorded at stations of the Global Seismograph Network (GSN), in epicentral distances from 30° to 90°. First motion *P*-waves polarities, recorded at distances less than 30°, were additionally used to have a better constrain on the solution.

A FIR (Finite Impulse Response) band pass filter was initially applied to the data (Oppenheim and Schafer, 1989), in order to remove the high frequency noise. The corner frequencies of this filter were determined by visually comparing the FFT spectra of the signal to those of the noise. For most cases the valuable frequency content of the waveforms was approximately lying in the frequency band f_1 = 0.02-0.01 Hz to f_2 = 0.2-0.3 Hz. Thus, these frequencies were used as the corner frequencies of the filter. All waveforms were converted into displacement, when it was necessary.

Synthetics were generated for a point source, buried in a half space. We used a *P*-wave velocity of 6.5 km/s, *S*-wave velocity of 3.7 km/s and density 2.6 g/cm^3. Receiver structure is assumed to be a homogenous half-space. The Source Time Function (STF), is described by the amplitudes of a series of overlapping isosceles triangles, the number and duration of which we selected *a priori*. The inversion routine yields amplitudes for each triangular shape. Amplitudes were adjusted for geometrical spreading, a simple function of epicentral distance (Langston and Helmberger, 1975), and for attenuation using Futterman's (1962) operator with t^* = 1 s for *P* and t^* = 4 s for *SH*-waves. The inversion returns the «minimum misfit solution» for the strike, dip, rake, depth and scalar seismic moment between the synthetics and the observed seismograms, in a weighted least square's sense. As it has been shown that the covariance matrix associated with the «minimum misfit solution» usually underestimates the true uncertainties, we followed the procedure of McCaffrey and Nabelek (1987) and Molnar and Lyon-Caen (1989) to find more realistic uncertainties. In this procedure one simply fixes the source parameters at values close to those yielded by the «minimum misfit solution» allowing all the others to vary during the inversion. The errors are found by visually examining when the match of the observed to synthetic seismograms significantly deteriorates.

3. Focal mechanisms of the major events of the sequence

The focal mechanism solutions obtained by the inversion, together with the associated uncertainties, are summarized in table I. In the following we briefly discuss the results for each earthquake studied.

3.1. *The 17 August 1999 Izmit mainshock M_w 7.4*

28 *P*- and 22 *SH*- waveforms with very good coverage in all azimuths were used in the inversion, and the results are shown in fig. 2. Even though a two-point source improved the fit in the *P*-wave waveforms, we prefer to keep the modelling of the single-point source, since the results show that one source is adequate to model the main rupture episode of this event. First motion polarities from 11 stations at distances < 30° (insets at the top of fig. 2) are in very good agreement with the solution returned by the inversion. The focal mechanism of the Izmit mainshock indicates dextral strike slip motion (rake = – 175°) on a nearly vertical fault with an E-W trend. Our solution is not far from the

Table I. Focal mechanism parameters and their uncertainties for the five earthquakes modelled using body wav modelling. Epicentres are taken from Kandili Observatory.

							1st Plane				2nd Plane			*P* Axis	*T* Axi
No.	Date Y/M/D	Time H:M	Lat. (°)	Long. (°)	M_w	$M_0 \times 10^{17}$ Nm	Depth (km)	Strike (°)	Dip (°)	Rake (°)	Strike (°)	Dip (°)	Rake (°)	Az/Pl (°)	Az/Pl (°)
1	990817	00:01	40.76	29.97	7.4	1311	10 (±2)	267 (±2)	85 (±1)	−175 (±3)	177	85	−5	132/7	222/0
2	990831	08:10	40.75	29.92	5.1	0.474	15 (±2)	82 (±15)	78 (+5/−1)	−141 (±15)	343	52	−15	310/35	207/1
3	990913	11:55	40.80	30.03	5.7	4.901	16 (+1/−2)	268 (±5)	49 (+2/−5)	180 (+5/−15)	359	89	41	126/27	232/2
4	991111	14:41	40.81	30.20	5.6	2.64	13 (±3)	297 (±5)	55 (±1)	−179 (±10)	206	89	−35	156/25	257/2
5	991112	16:57	40.79	31.21	7.1	470.8	12 (±3)	262 (±5)	53 (±2)	−177 (±3)	170	88	−37	119/27	222/2

Harvard CMT one, which is shown for comparison (bottom of fig. 2). The synthetics produced by the CMT solution (strike, dip and rake fixed, all other parameters free) fail to predict the polarity at KMI and TSUM, and indicate poor amplitude fitting for most stations.

3.2. *The 31 August 1999 aftershock M_w 5.1*

This is a moderate size aftershock ($M_w = 5.1$) which was recorded with high signal to noise ratio in a small number of stations. The inversion was based on 5 *P*- and 16 *SH*-waveforms, shown in fig. 3, and was additionally constrained by 11 *P*-wave first motion polarities from stations at distances < 30° (insets in fig. 3). Some of these stations were close to the node thus the NNW-SSE trending nodal plane is well constrained. The Harvard CMT solution (NP1: strike = 77°, dip = 78°, slip = −121°; NP2: strike = 329°, dip = 33°, rake = −22°, h = 15 km) is in agreement with our solution. This aftershock is associated with dextral strike-slip motion with a small normal component.

3.3. *The 13 September 1999 aftershock M_w 5.7*

31 *P*- and 19 *SH*-waveforms were used in the inversion with a good coverage in terms of azimuth. All waveforms had high signal/noise ratios and allowed the calculation of synthetics with a very good fit to the observed waveforms (fig. 4). The solution obtained indicates pure dextral strike slip motion along an ~E-W striking plane dipping to the north. First motion polarities at 9 stations from distances < 30° (insets in fig. 4) were very important in constraining the nodal planes since most of them were close to the node (*i.e.* KIEV, OBN). The inversion yielded a short time function for this event (~2.5 s) in contrast with the STF's of the other aftershocks modelled here, which were longer (~6-7 s on average). Our solution differs from the Harvard CMT solution as far as the dip angle of the northward dipping plane is concerned. The synthetics produced using the CMT Harvard solution (bottom of the fig. 4) deteriorate the fit especially for the horizontal components (stations CHTO, FFC, ALE).

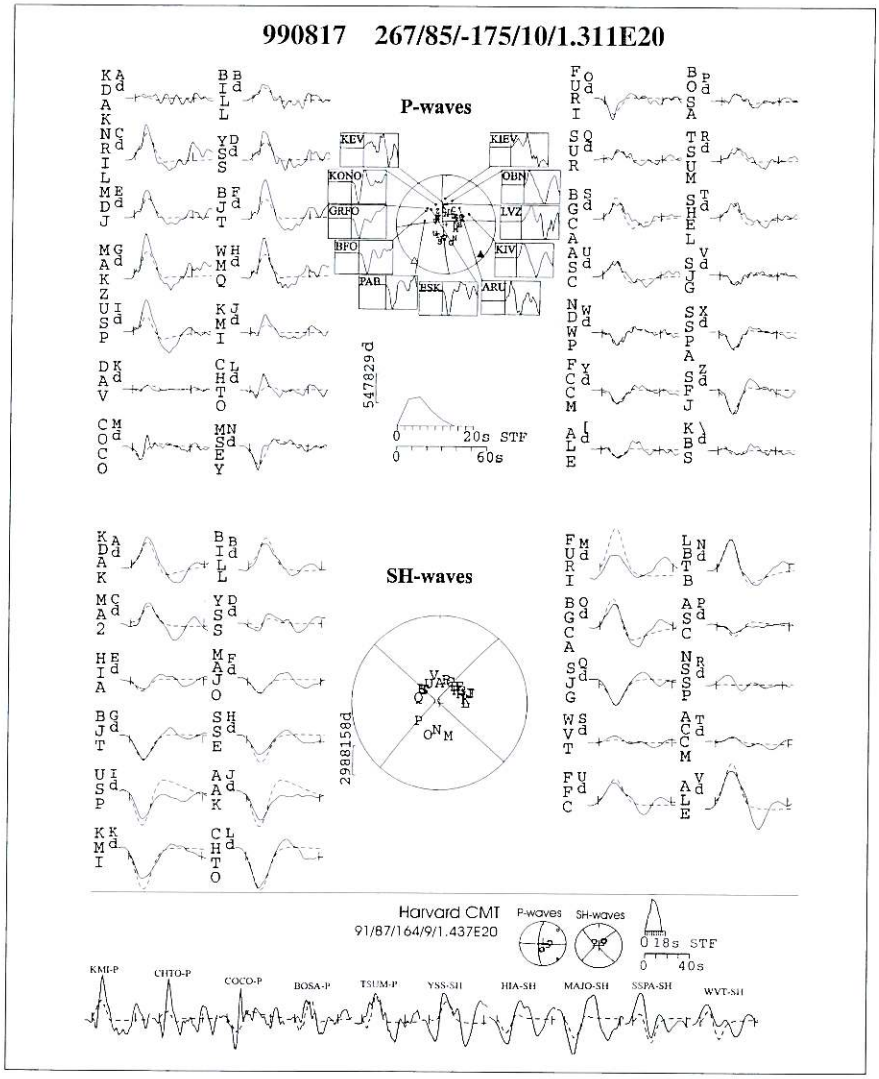

Fig. 2. The *P* and *SH* radiation patterns of the minimum misfit solution for the August 17, 1999 earthquake. The values beneath the event header give strike, dip, rake (in degrees), the depth (in km) and the seismic moment (in Nm). The focal spheres are shown with the *P* and *SH* nodal planes in lower hemisphere projections. The *P* and *T* axes are marked by solid and open triangles, respectively. The observed *P* and *SH* waveforms (solid lines) are compared with synthetic waveforms (dashed lines) computed for the minimum misfit solution. These are ordered clockwise by azimuth and the station code of each waveform is accompanied by a letter corresponding to its position within the focal sphere. The waveform amplitudes are normalized at a distance of 40° and a gain of 6000. Solid bars at either end of the waveform mark the inversion window. The source time function is shown below the *P*-wave focal sphere, with the waveform time scale below this. Waveform amplitude scales (in microns) are to the left of the focal sphere. The insets show the first motion polarities at stations at distances < 30°, which were not used in the inversion, but only complimentary used to constrain the nodal planes. In the lower part we show the comparison between synthetics (dashed lines) and observed (solid lines) seismograms for *P* and *SH* waves produced for the Harvard CMT solution.

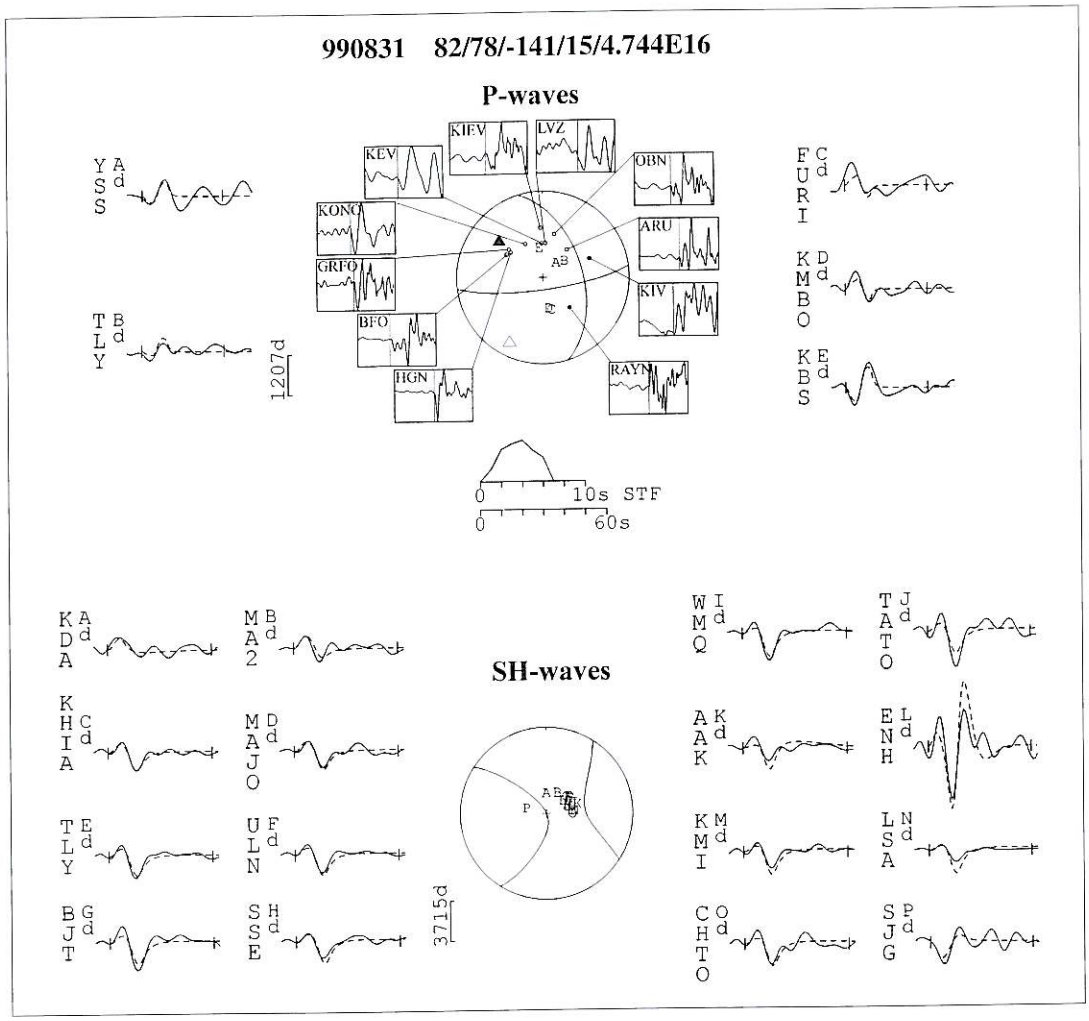

Fig. 3. The same as in fig. 2 for the event of August 31, 1999.

3.4. *The 11 November 1999 aftershock M_w 5.6*

25 *P*- and 23 *SH*-waveforms, adequately recorded at all azimuths, were used in the inversion and are shown in fig. 5. The solution obtained indicates strike slip motion. First motion *P*-wave polarities from 11 stations, from distances $< 30°$, were additionally used to constrain the WNW-ESE trending plane (insets in fig. 5). The Harvard CMT solution for this event (NP1: strike = 301°, dip = 50°, rake = −175°; NP2: strike = 208°, dip = 86°, slip = −41°, h = = 15 km) is not significantly different from the one we obtained.

3.5. *The 12 November 1999, Bolu mainshock M_w 7.1*

The epicentre of this earthquake is located ~110 km east of the Izmit event (fig. 1). 26 *P*- and 24 *SH*-waveforms were used in the inver-

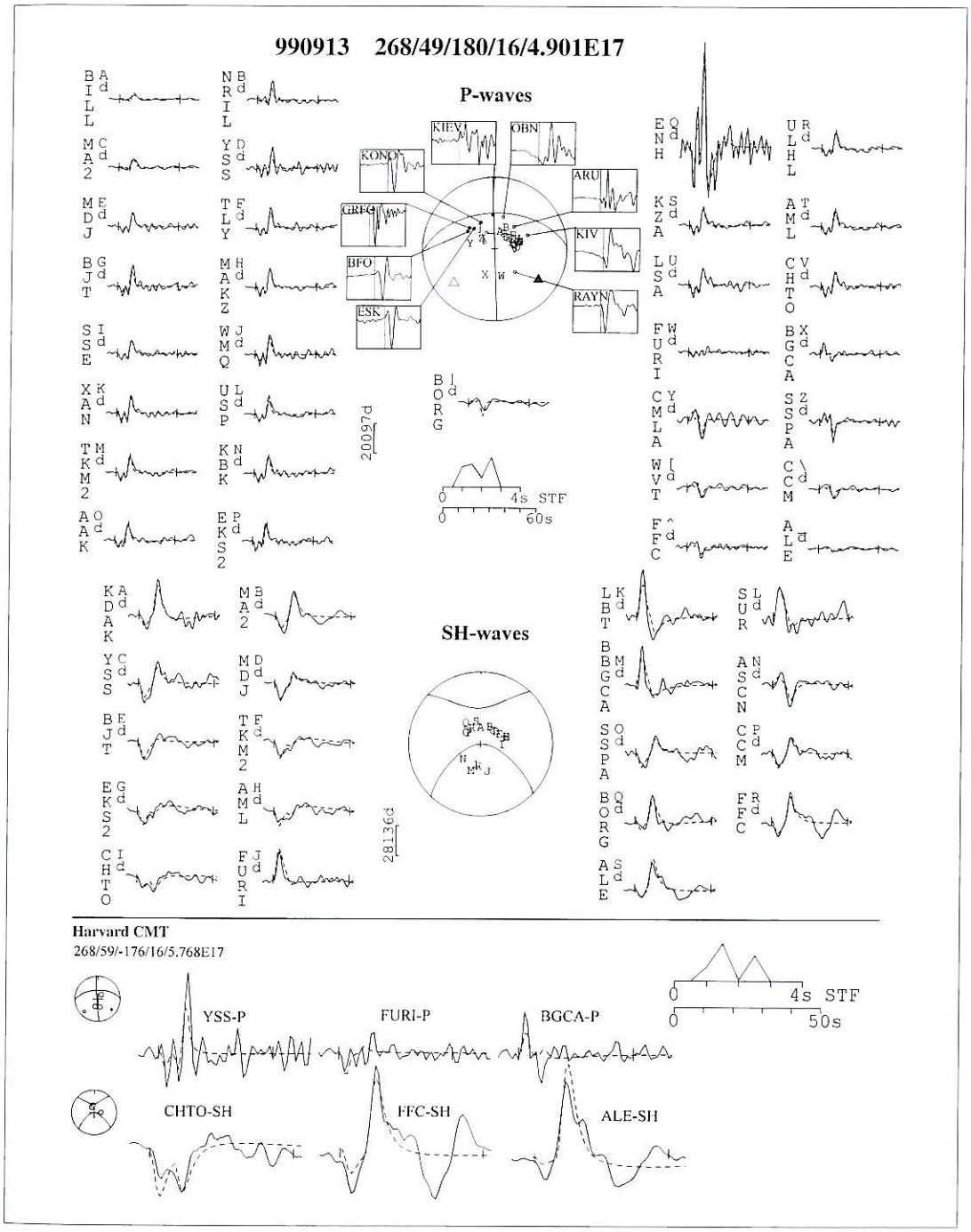

Fig. 4. The same as in fig. 2 for the event of September 13, 1999.

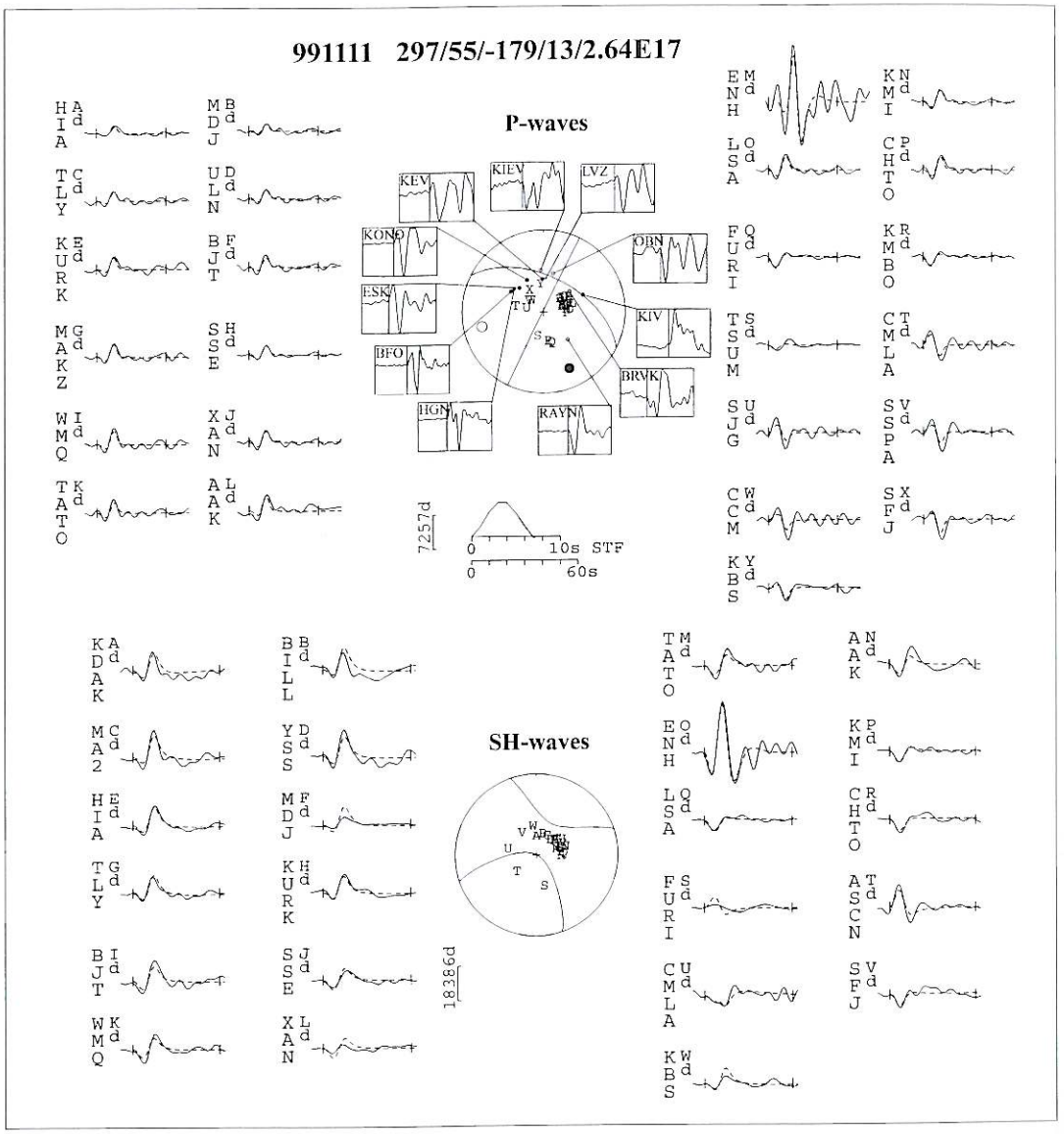

Fig. 5. The same as in fig. 2 for the event of November 11, 1999.

sion. Figure 6 shows the match between the observed seismograms and synthetic *P* and *SH* seismograms computed for the minimum misfit solution. This solution indicates dextral strike slip motion along a ~ E-W trending plane that dips at 53° towards the north. Both nodal planes are well constrained and in agreement with the first motion polarities from 11 stations at distances < 30°. The source time function, with a total duration of 13 s, has a characteristic shape consisting of two pulses, which are visible at the *P*-waveforms in nearly all azimuths. The Har-

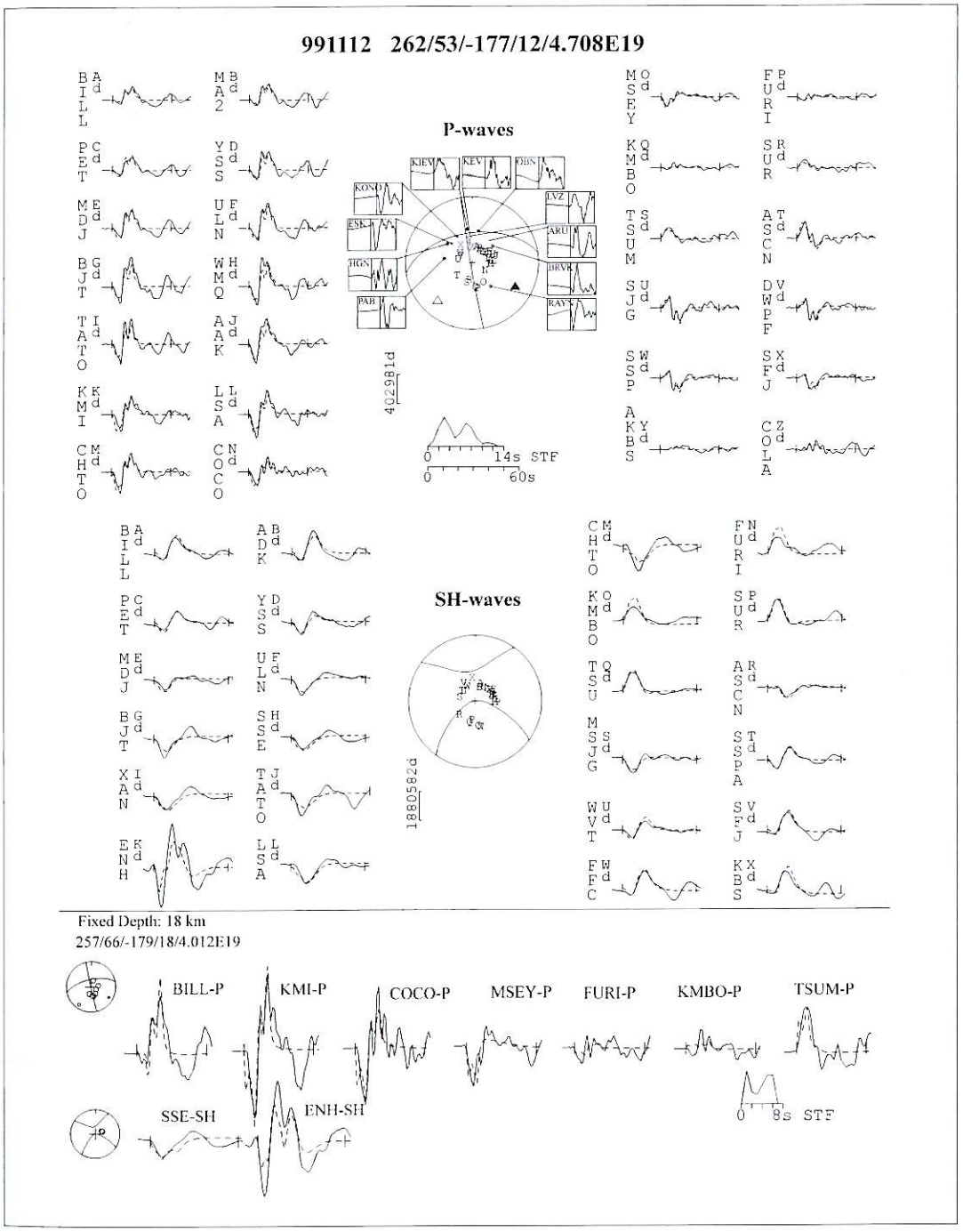

Fig. 6. The same as in fig. 2 for the event of November 12, 1999.

vard CMT solution is not considerably different from the one that we obtained as far as the parameters of the focal mechanism are concerned. However we differ in the depth estimate for this event. Our focal depth estimate is 12 km in contrast with the Harvard estimate which is 18 km. The lower part of fig. 6 compares selected *P* and *SH* waveforms computed using a depth fixed at 18 km. We clearly observe that a deeper source significantly deteriorates the fitting.

4. Source parameters from far-field displacement spectra

Source parameters, such as moment (M_0), fault length (L), fault width (W), average displacement ($\bar{u}$) across the fault and static stress drop ($\Delta\sigma$), were determined for the two largest earthquakes of August 17 and November 12, 1999, using the far-field displacement amplitude spectra. The data used consist of *P*-waves (with sampling frequency of 1 Hz) recorded at teleseismic distances 30°-90° from the GSN stations. The displacement waveforms were corrected for the instrument response, the radiation pattern, and attenuation. The radiation pattern was calculated for each station used, based on the fault plane solution obtained from the previous analysis. For the stations that were close to the node, that normally have a radiation pattern less than 0.1, we did not attempt to calculate seismic moment, because it would be too large (Hanks and Wyss, 1972). The time window was

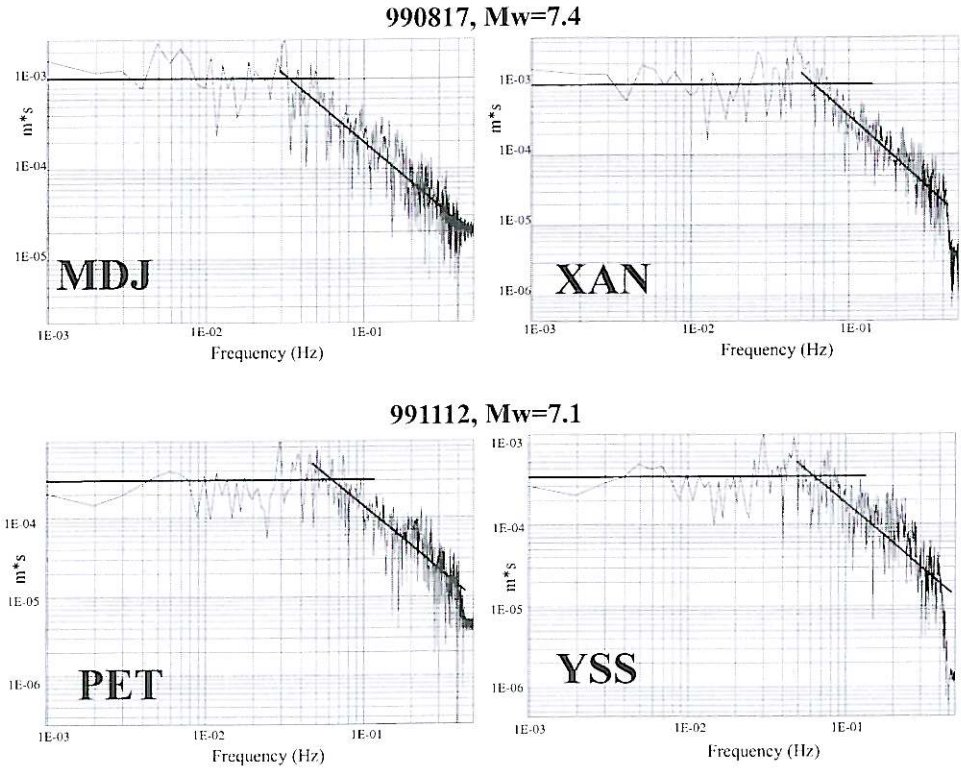

Fig. 7. Far-field displacement amplitude spectra for the August 17, 1999 and the November 12, 1999 earthquakes. Displacement waveforms have been corrected for instrument response, attenuation, and the radiation pattern. The low and high frequency asymptotes (straight lines) were fitted by eye.

carefully selected starting at the *P*-arrival and ending before the *S*-arrival.

Figure 7 shows the displacement amplitude spectra for two stations for the August 17 event and the November 12, 1999 event. The far-field spectrum is characterised by 3 parameters: i) the low-frequency level, Ω_0, which is proportional to seismic moment; ii) corner frequency, f_c, and iii) the power of the high-frequency asymptote. Following Brune (1970, 1971), we shall define

Table IIa,b. Station parameters (station code, distance, azimuth, radiation pattern) used in the analysis and spectral parameters (Ω_0, f_c) obtained from the *P*-wave far-field displacement spectra for the August 17, 1999 (a) and the November 12, 1999 (b) earthquakes. Stations that were close to the node and have $\Re_{\theta\varphi} < 0.1$, are marked with an asterisk, and were not used in the seismic moment calculation.

(a) Earthquake of August 17, 1999

Station code	Distance (km)	Az. (°)	$\Re_{\theta\varphi}$	Ω_0 (m-s)	f_c (Hz)
BILL	4354	16	0.176	5.72E-04	0.051
NRIL	2673	27	0.309	1.44E-03	0.055
MA2	4943	28	0.206	1.01E-03	0.039
YSS	5977	41	0.203	9.33E-04	0.054
HIA	4783	49	0.252	1.23E-03	0.062
MDJ	5632	49	0.219	9.81E-04	0.033
MAJO	6840	51	0.180	5.64E-04	0.067
BJT	5342	59	0.214	1.39E-03	0.048
MAKZ	3035	63	0.283	1.90E-03	0.059
SSE	6401	65	0.169	4.79E-04	0.046
WMQ	3485	66	0.253	1.91E-03	0.05
XAN	5394	68	0.182	9.35E-04	0.059
TATO	6979	69	0.141	5.56E-04	0.072
USP	2741	70	0.239	1.93E-03	0.043
TKM2	2819	71	0.234	1.91E-03	0.049
KBK	2790	71	0.230	1.88E-03	0.054
AAK	2764	71	0.229	1.88E-03	0.046
EKS2	2720	71	0.228	1.92E-03	0.053
ULHL	2883	72	0.224	1.91E-03	0.06
KZA	2830	72	0.220	1.87E-03	0.062
KMI	5696	80	0.113	6.32E-04	0.057
LSA	4554	82	0.113	9.20E-04	0.061
FURI	3217	163	0.161	4.51E-04	0.099
BGCA*	3666	199	0.084	7.51E-04	0.062
ASCN*	6524	231	0.067	9.62E-04	0.036
SJG*	7885	287	0.077	3.70E-04	0.048
DWPF*	7852	304	0.075	4.60E-04	0.048
SSPA*	6368	312	0.097	4.86E-04	0.048
WVT*	7319	314	0.070	4.75E-04	0.044
CCM*	7261	317	0.063	4.48E-04	0.046
SFJ	3276	330	0.119	5.94E-04	0.066

(b) Earthquake of November 12, 1999

Station code	Distance (km)	Az. (°)	$\Re_{\theta\varphi}$	Ω_0 (m-s)	f_c (Hz)
BILL	4307	17	0.320	4.04E-04	0.046
MA2	4878	28	0.409	4.90E-04	0.045
PET	5790	30	0.377	4.01E-04	0.056
YAK	4077	33	0.493	6.14E-04	0.041
YSS	5890	42	0.452	5.01E-04	0.055
HIA	4692	49	0.560	7.38E-04	0.072
MDJ	5536	50	0.512	5.01E-04	0.047
TLY	3797	51	0.627	8.15E-04	0.055
ULN	4189	55	0.613	5.58E-04	0.071
KURK	2642	57	0.698	6.45E-04	0.075
BJT	5237	60	0.554	7.91E-04	0.056
MAKZ	2937	63	0.672	8.03E-04	0.090
SSE	6287	66	0.504	3.08E-04	0.078
WMQ	3382	66	0.647	1.00E-03	0.089
XAN	5282	69	0.550	6.24E-04	0.081
AAK	2660	72	0.650	7.81E-04	0.095
ENH	5617	73	0.526	6.21E-04	0.067
LSA	4439	83	0.531	7.48E-04	0.072
KMBO*	4286	171	0.015	2.44E-04	0.091
SUR*	7825	189	0.032	3.06E-04	0.051
TSUM*	6435	195	0.053	4.04E-04	0.057
ASCN	6629	232	0.235	4.10E-04	0.056
SJG	7976	288	0.332	1.99E-04	0.070
SSPA	6419	312	0.293	2.21E-04	0.072
CCM	7304	318	0.214	2.02E-04	0.062
SFJ	3294	330	0.272	3.06E-04	0.065
KBS*	2174	354	0.073	2.08E-04	0.081

the corner frequency at the intersection of the low- and high-frequency asymptotes in the spectrum. Two models are usually used for the high-frequency asymptote, the ω-square, and the ω-cube (Aki and Richards, 1980). For instance, for bilateral faulting with rupture velocity, v and final fault length, L (Savage, 1972) the high frequency asymptote is proportional to ω^{-2}. We determined the spectral parameters (Ω_0, f_c) by eye fitting low- and high- frequency asymptotes to the observed spectra and these are listed in table II.

Scalar seismic moment, M_0, was calculated from the relation (Keilis-Borok, 1960)

$$M_0(P) = \frac{\Omega_0(P)}{\Re_{\theta\varphi}(P)} 4\pi\rho R a^3 \qquad (4.1)$$

where $\Omega_0(P)$ denotes the low-frequency spectral level of the P-wave, ρ is the density (= 2.6 g/cm^3), $\Re_{\theta\varphi}(P)$ is the radiation pattern for the P-wave, R is the epicentral distance, in km, and a is the P-wave velocity (= 6.5 km/s).

We considered a rectangular fault of width, W, and length, L (Savage, 1972). The width, W, was assumed equal to 15 km (based on the distribution of aftershocks, and Yagi and Kikuchi 1999, 2000 modelling) and then the length, L, of the fault was calculated from the relation (Aki and Richards, 1980)

$$\sqrt{LW} = \frac{a\sqrt{2.9}}{2\pi f_{c_P}}. \qquad (4.2)$$

Static stress drop, $\Delta\sigma$, was calculated from the relation

$$\Delta\sigma = \frac{2M_0}{\pi L W^2} \qquad (4.3)$$

(Knopoff, 1958; Kanamori and Anderson, 1975) that holds for strike-slip faults. The average displacement, $\bar{u}$, across the fault is calculated from the relation (Aki, 1966)

$$M_0 = \mu A \bar{u} \qquad (4.4)$$

where μ is the shear modulus (= $3.3 \cdot 10^{10}$ N/m^2) and A is the fault surface, in km^2.

Table III lists the source parameters determined from the spectral analysis for the two earthquakes studied.

5. Conclusions - Discussion

Body waveform modelling was used to obtain the focal mechanism of five events of the Izmit-Bolu 1999 sequence in Turkey. Far-field P-wave spectral analysis was also performed to determine the source parameters for the Izmit August 17, 1999 and the Bolu November 12, 1999 mainshocks.

The results show that all five earthquakes were connected with dextral strike-slip motion on planes that strike ~ E-W, following the strike of the North Anatolian Fault Zone. Focal depths for these events range from 10 to 16 km.

The focal mechanism for the August 17, 1999 event indicates pure strike-slip motion on a nearly vertical plane. The derived mechanism (strike 267°, dip 85°, rake – 175°) is in agreement with the results of similar studies (Bouchon *et al.*, 2000; Ayhan *et al.*, 2001; Tibi *et al.*, 2001; Thio and Polet, 1999; Toksöz *et al.*, 1999; Örgulu and Aktar, 1999 among other references in the *Abstract Book of the AGU 1999, Fall Meeting*). From far-field spectral analysis the length of the fault was found equal to 76 km, in accordance with the results of Yagi and Kikuchi (2000) who obtained a value of 70 km from the joint in-

Table III. Source parameters of the two large events as derived from far-field spectral analysis.

Earthquake	Moment ($\times 10^{17}$ Nm)	Stress drop (bar)	Length (km)	Width (fix) (km)	Displacement (cm)
17 August 1999	2090 (±578)	90 (±38)	76 (±35)	15	640 (±268)
12 November 1999	491 (±167)	29 (±11)	56 (±27)	15	205 (±82)

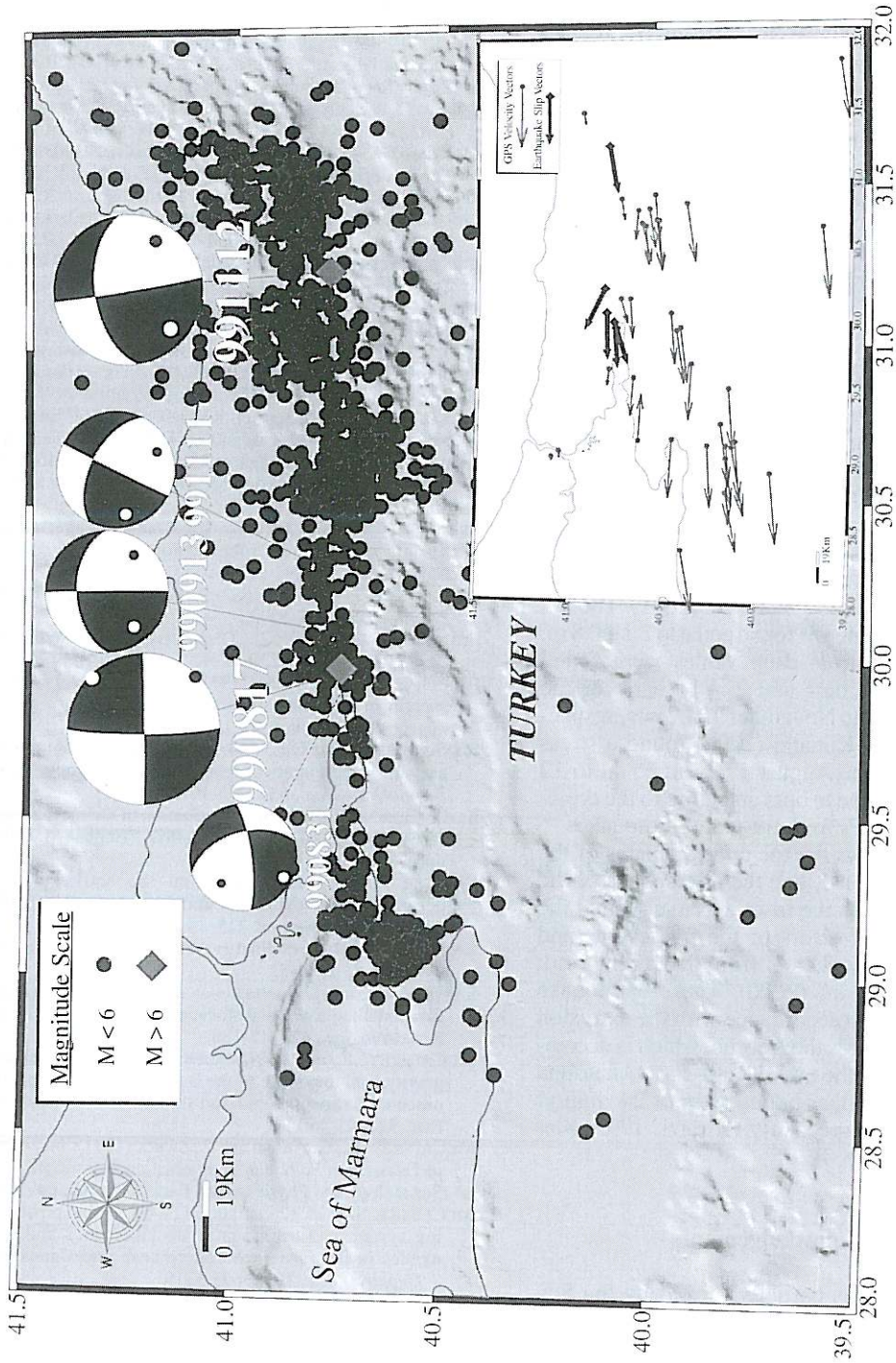

Fig. 8. Aftershock locations of the Izmit-Bolu sequence (data from Kandili Observatory) and the focal mechanisms determined by us. The inset shows the earthquake slip vectors (horizontal projection) of the five events studied and the GPS velocity vectors from McClusky *et al.* (2000). Earthquake slip vectors are in agreement with the westward motion of Anatolia.

version of near-field and teleseismic data. The average displacement was found equal to 6.4 ± 2.7 m, similar to the maximum dislocation of 6.3 m determined by Yagi and Kikuchi (2000). The measured offsets at the surface were about 2.5 to 3.5 m with a maximum of 5 m (USGS field reports; Barka *et al.*, 1999). As indicated by Barka and his colleagues (1999), the surface rupture of the August 17, 1999 event consisted of four different right stepping segments between Düzce and Karamursel. The maximum displacement of 5 m was observed in the Sapanca-Akyazi segment. Local vertical displacements of up to 1-2 m occurred where the surface rupture stepped over.

The Bolu November 12, 1999 event was associated with dextral strike slip motion along an ENE-WSW trending fault segment, with a smaller dip angle (dip = 53°) with respect to the Izmit fault plane (dip = 85°). The length of the fault was found equal to 56 km, in accordance with the fault ruptures and the modelling of Yagi and Kikuchi (1999) and Ayhan *et al.* (2001). The average displacement was found equal to 2.1 ± 0.8 m. Average static stress drop values were found equal to 90 ± 38 bars and 29 ± 11 bars for the August 17 and the November 12 events, respectively. Yagi and Kikuchi (2000) found a stress drop value for the August 17 event equal to 12 MPa, a value close to ours and close to the typical value of 10 MPa for intra-plate earthquakes.

Figure 8 shows the focal mechanisms of the earthquakes studied, and the aftershocks of the 1999 sequence. In the inset we have plotted the earthquake slip vectors of the five events and the GPS velocity vectors from the recent work of McClusky *et al.* (2000). These earthquake slip vectors are in accordance with the extrusion of Anatolia towards the Aegean, which is accommodated along the North and East Anatolian Fault Zones at upper bound rates of 24 mm/yr and 9 mm/yr, respectively (Kiratzi, 1993; McClusky *et al.*, 2000).

Acknowledgements

This work was partially funded by the Science for Peace Project (SfP 972342) and by OASP of Greece (Project 20246).

REFERENCES

AKI, K. (1966): Generation and propagation of *G*-waves from the Niigata earthquake of June 16, 1964. Part 2. Estimation of earthquake moment, released energy, and stress-strain drop from the *G*-waves spectrum. *Bull Earthquake Res. Inst., Tokyo Univ.*, **44**, 73-88.

AKI, K. and P. RICHARDS (1980): *Quantitative Seismology: Theory and Methods* (Freeman, San Francisco, Calif.), pp. 557.

AYHAN, M., R. BÜRGMANN, S. MCCLUSKY, O. LENK, B. AKTUG, E. HERECE and R. REILINGER (2001): Kinematics of the M_w = 7.2, 12 November 1999, Düzce, Turkey earthquake. *Geophys. Res. Lett.*, **28**, 367-370.

BARKA, A.A. (1992): The North Anatolian fault zone. *Ann. Tectonicae*, **6**, 164-195.

BARKA, A. *et al.* (1999): 17 August 1999 Izmit earthquake, Northwestern Turkey, *Book of Abstracts of the AGU 1999 Fall Meeting*.

BOUCHON, M., N. TOKSOZ, H. KARABULUT, M.-P. BOUIN, M. DIETRICH, M AKTAR and M. EDIE (2000): Seismic imaging of the 1999 Izmit (Turkey) rupture inferred from the near-fault recordings, *Geophys. Res. Lett.*, **27**, 3013-3016.

BRUNE, J.N. (1970): Tectonic stress and the spectra of seismic shear waves from earthquakes. *J. Geophys. Res.*, **75**, 4997-5009.

BRUNE, J.N. (1971): Correction (to Brune, 1970), *J. Geophys. Res.*, **76**, 5002.

FUTTERMAN, W.I. (1962): Dispersive body waves, *J. Geophys. Res.*, **67**, 5279-5291.

HANKS, T.C. and M. WYSS (1972): The use of body-wave spectra in the determination of seismic-source parameters, *Bull. Seismol. Soc. Am.*, **62**, 561-589.

KANAMORI, H. and D.L. ANDERSON (1975): Theoretical basis of some empirical relations in seismology, *Bull. Seismol. Soc. Am.*, **65**, 1073-1095.

KEILIS-BOROK, V.I. (1960): Investigation of the mechanism of earthquakes, *Sov. Res. Geophys.* (English translation), **4**, 29.

KIRATZI, A. (1993): A study on the active crustal deformation on the North and East Anatolian Fault Zones, *Tectonophysics*, **225**, 191- 203.

KNOPOFF, L. (1958): Energy release in earthquakes, *Geophys. J.*, **1**, 44-52.

LANGSTON, C. and D.V. HELMBERGER (1975): A procedure for modelling shallow dislocation sources, *Geophys. J. R. Astron. Soc.*, **42**, 117-130.

MCCAFFREY, R. and J. NABELEK (1987): Earthquakes, gravity, and the origin of the Bali basin: an example of nascent continental fold-and-thrust belt, *J. Geophys. Res.*, **92**, 441-460.

MCCAFFREY, R., G. ABERS and P. ZWICK (1991): *Inversion of Teleseismic Body Waves*, International Association of Seismology and Physics of the Earth's Interior, pp. 166.

MCCLUSKY, S. *et al.* (28 authors) (2000): Global positioning system constraints on plate kinematics and dynamics in the Eastern Mediterranean and Caucasus, *J. Geophys. Res.*, **105**, 5695-5719.

MOLNAR, P. and H. LYON-CAEN (1989): Fault plane solutions of earthquakes and active tectonics of the Tibe-tan Plateau and its margins, *Geophys. J. Int.*, **99**, 123-153.

OPPENHEIM, A.V. and R.W. SCHAFER (1989): *Discrete-Time Signal Processing* (Prentice Hall, U.S.A.), pp. 879.

ÖRGÜLÜ, G. and M. AKTAR (1999): Regional moment tensor analysis of the aftershocks of the Izmit earthquake (8/17/1999 M_w = 7.4), *Book of Abstracts of the AGU 1999 Fall Meeting*.

PAPAZACHOS, B.C., E.E. PAPADIMITRIOU, A.A. KIRATZI, C.B. PAPAZACHOS and E.K. LOUVARI (1998): Fault plane solutions in the Aegean Sea and the surrounding area and their tectonic implication, *Boll. Geofis. Teor. Appl.*, **39**, 199-218.

SAVAGE, J.C. (1972): Relation of corner frequency to fault dimensions, *J. Geophys. Res.*, **77**, 3788-3795.

STEIN, R.S., A.A. BARKA and H. JAMES (1997): Progressive failure on the North Anatolian fault since 1939 by earthquake stress triggering, *Geophys. J. Int.*, **128**, 594-604.

THIO, H.K. and J. POLET (1999): Rupture complexity of the 1999 Izmit earthquake, *Book of Abstracts of the AGU 1999 Fall Meeting*.

TIBI, R., G. BOCK, Y. XIA, M. BAUMBACH, H. GROSSER, C. MILKEREIT, S. KARAKISA, S. ZÜNBÜL, R. KIND and J. ZSCHAU (2001): Rupture process of the 1999 August 17 Izmit and November 12 Düzce (Turkey) earthquakes, *Geophys. J. Int.*, **144**, F1-F7.

TOKSÖZ, M.N., A.F. SHAKAL and A.J. MICHAEL (1979): Space-time migration of earthquakes along the North Anatolian fault zone and seismicity gaps, *Pure Appl. Geophys.*, **117**, 1258-1270.

TOKSÖZ, N., R. REILINGER, C. DOLL, A. BARKA and N. YALCIN (1999): Izmit (Turkey) earthquake of 17 August 1999: first report, *Seismol. Res. Lett.*, **70**, 669-679.

YAGI, Y. and M. KIKUCHI (1999): *Preliminary Results of Rupture Process for the November 12, 1999 Turkey Earthquake* (http://wwweic.eri.utokyo.ac.jp).

YAGI, Y. and M. KIKUCHI (2000): Source rupture process of the Kocaeli, Turkey, earthquake of August 17, 1999, obtained by joint inversion of near-field data and teleseismic data, *Geophys. Res. Lett.*, **27**, 1969-1972.

(received March 14, 2000;
accepted November 30, 2000)